Structure of C8α-MACPF Reveals Mechanism of Membrane Attack in Complement Immune Defense

Michael A. Hadders, Dennis X. Beringer, Piet Gros*

Membrane attack is important for mammalian immune defense against invading microorganisms and infected host cells. Proteins of the complement membrane attack complex (MAC) and the protein perforin share a common MACPF domain that is responsible for membrane insertion and pore formation. We determined the crystal structure of the MACPF domain of complement component C8α at 2.5 angstrom resolution and show that it is structurally homologous to the bacterial, pore-forming, cholesterol-dependent cytolysins. The structure displays two regions that (in the bacterial cytolysins) refold into transmembrane β hairpins, forming the lining of a barrel pore. Local hydrophobicity explains why C8α is the first complement protein to insert into the membrane. The size of the MACPF domain is consistent with known C9 pore sizes. These data imply that these mammalian and bacterial cytolytic proteins share a common mechanism of membrane insertion.

Protection in blood against Gram-negative bacteria critically depends on the cytolytic activity of the terminal pathway of the complement system (*1*, *2*). Deficiency in components of the terminal pathway results in recurrent bacterial infections in humans [in particular, meningococcal infections (*3*)]. The terminal pathway is initiated when complement protein C5 is proteolytically activated into two fragments, C5a and C5b, in the complement cascade (*4*). C5b then sequentially binds C6, C7, C8, and multiple copies of C9, forming a C5b–9 complex called the MAC. The complement proteins C6 to C9 are homologous and have a central MACPF domain of molecular mass ~40 kD, flanked by small regulatory domains at the N and C termini (fig. S1) (*5*). C8 is a trimer made up of homologous proteins C8α and C8β, each of which contain a MACPF domain, and a lipocalin protein C8γ that is covalently linked to C8α through a disulfide bridge (*6*). During assembly of the MAC, C7 mediates the initial binding to the membrane surface. However, the C8α component of C8 is the first protein that traverses the lipid bilayer (*7*, *8*). C5b–8 complexes, obtained in the absence of C9, have hemolytic activity, indicating that C8 penetration leads to a loss of membrane integrity (*9*). After C5b–8 assembly, multiple C9 molecules bind and oligomerize into pores, consisting of 12 to 18 C9 monomers, that are 100 ± 10 Å wide and 160 Å high (*10*–*12*). Host cells are protected from this membrane attack by CD59, which binds to C8α and C9 during MAC assembly, preventing pore formation (*13*). Cytotoxic T lymphocytes and natural killer cells secrete granules containing perforin, which (like the complement proteins C6 to C9) has a central MACPF domain. Perforin multimerizes, forming similar pores composed of ~20 monomers (*14*–*16*). Perforin, however, does not use accessory proteins for membrane binding (*16*). The mechanism of membrane insertion and pore formation by these proteins of the immune system is unclear.

We expressed and crystallized the human C8α-MACPF domain (residues 103 to 462). The C8α-MACPF domain retains its ability to form heterotrimeric C8 (with full-length C8β and C8γ) that is functionally active in membrane attack and pore formation (*17*). The structure was determined to 2.5 Å resolution by experimental phasing (see the Materials and Methods, table S1, and fig. S2 in the supporting online material). The overall structure consists of a central kinked four-stranded β sheet surrounded by α helices and β strands, forming two structural segments (which we call d1 and d3 for reasons discussed below) (Fig. 1A). Overall, the molecule has a thin L-shaped appearance with dimensions 67 Å by 55 Å by 24 Å.

The observed fold of C8α-MACPF with its central kinked β sheet resembles the fold of domains d1 and d3 of intermedilysin and perfringolysin, which are cholesterol-dependent cytolysins (CDCs) secreted by the Gram-positive bacteria (*18*, *19*) (Fig. 1B and fig. S3). CDCs undergo substantial refolding of part of their structure in transforming from monomeric soluble proteins to multimeric membrane pores [reviewed in (*20*)]. CDCs are built up of four domains: d1 to d4. Domain d4 is responsible for membrane binding (*21*, *22*), whereas d2 forms a linker to d1 and d3, which mediate pore formation (*23*). Domains d1 and d3 correspond to the two halves of the kinked β sheet in the structure of C8α-MACPF, which is consistent with the membrane-insertion function of C8α-MACPF. The absence of the d2 and d4 domains in C8α-MACPF correlates, however, with marked topological differences in d1 (fig. S3, C and D). The modules flanking the C8α-MACPF domain [that is, the N-terminal thrombospondin type 1 (TSP1) and low-density lipoprotein receptor class a domains and the C-terminal epidermal growth factor–like and TSP1 domains] are linked on opposite sides to d1 (Fig. 1A). The covalent binding site for C8γ (Cys^{164}) is located in a disordered surface loop on the N-terminal side of d1. In contrast, the topologies of d3 in C8α and CDCs are very similar and are characterized by an antiparallel β sheet (strands β1 to β4) with extended, connecting regions β1-β2 and β3-β4.

Residues from domain d3 in CDCs form the wall of the β barrel pores. In CDCs, the antiparallel β sheet (strands β1 to β4) in d3 has two helical connections (between strands β1-β2 and β3-β4). By means of multiple spectroscopic methods, these two helical regions have been shown to refold into amphipathic β hairpins [denoted transmembrane β hairpin 1 (TMH1) and TMH2], which insert into the membrane, forming a β barrel pore (*24*, *25*). C8α-MACPF

Crystal and Structural Chemistry, Bijvoet Center for Biomolecular Research, Department of Chemistry, Faculty of Science, Utrecht University, Padualaan 8, 3584 CH Utrecht, Netherlands.

*To whom correspondence should be addressed. E-mail: p.gros@chem.uu.nl

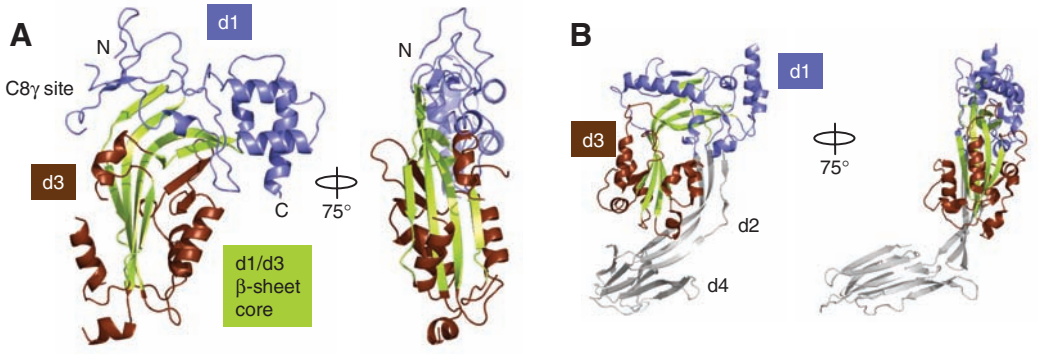

Fig. 1. Structure of human C8α-MACPF. Cα representation of C8α-MACPF (**A**) and intermedilysin (PDB accession code 1s3r) (**B**) in two views. The top and bottom halves of the molecule are denoted d1 (blue) and d3 (brown), respectively. The central kinked β sheet (part of both d1 and d3) is shown in green. The additional domains d2 and d4 in intermedilysin are shown in gray. Figures are produced with PyMOL (*30*).

exhibits similar, but longer, regions in between strands β1-β2 and β3-β4. The first region spans 58 residues (residues 201 to 258) and forms two α helices interspersed with a β hairpin (Fig. 2A). The second region consists of 62 residues (residues 326 to 387). This region has two discernible α helices in the electron density but is largely disordered. Like in CDCs, these regions show high sequence variation across species (fig. S4). In C8α, we observe a partitioning into three segments for these regions: (i) charged and amphipathic, (ii) hydrophobic, and (iii) charged and amphipathic (Fig. 2B and fig. S4). In the structure, the hydrophobic middle part (26 residues long) of region β1-β2 forms a β hairpin that aligns with the central sheet of d1. The corresponding part in region β3-β4 is 25 residues long and is delimited by the disulfide bond Cys^{345}-Cys^{369}. This hydrophobic part has three charged residues positioned halfway between the cysteine residues. The hydrophobic character of the central β1-β2 and β3-β4 parts is consistent with membrane insertion without pore formation, as expected for the function of C8. Presumably, the central β3-β4 part would traverse the membrane completely and position the three charged residues on the inside of the target membrane. In contrast, the central parts of the β1-β2 and β3-β4 regions in C9 and perforin (Fig. 2B and fig. S4) have an alternating hydrophobic and hydrophilic character (like the TMHs of CDCs). This amphipathic character is consistent with forming a β barrel pore with a hydrophilic inside and a hydrophobic outside that faces the lipid membrane. The flanking regions in C8α, C9, and perforin contain short stretches of consecutive charged residues indicative of a solvent-exposed character. We hypothesize that the central segments traverse the membrane (forming TMHs) and that the flanking parts protrude above the membrane.

Electron micrographs of the MAC and poly (C9) reveal a pore (~100 Å inner-diameter, ~160 Å height, and ~200 Å outer-diameter torus) and a small rim at the base of the pore (*12*). Our structure shows that a soluble, monomeric MACPF domain has a thin "L" shape. In analogy with CDCs, the β1-β2 and β3-β4 regions in d3 are expected to change into long β hairpins upon membrane insertion, contributing four strands per monomer. Extending 60 residues into one straight β hairpin yields a maximum length of ~100 Å; this structure would extend from the existing four-stranded β sheet in d3. Together with the MACPF domain, this yields a total length of ~160 Å, which is consistent with the height measured for MAC and C9 pores by electron microscopy (EM). Similarly, modeling of the x-ray structure of perfringolysin into a cryo-EM map of a pneumolysin pore also indicated extended β hairpins oriented parallel to the membrane normal (*26*). However, the β strands are most likely twisted and tilted (as observed in many β barrel structures of outer-membrane proteins); possibly, the missing N-terminal domains contribute to the height of the C9 pore. Furthermore, the putative TMH1 in C9 has a 17-residue extension, which is consistent with the presence of a small rim at the bottom side of the pore. Based on the MACPF domain of C8α, we constructed a hypothetical model of the C9 pore torus. Sixteen and 18 copies of the molecule were placed in rings, with the β1 to β4 strands of d3 placed on the inside (Fig. 3). This simplistic modeling resulted in rings with an inner diameter of 97 and 110 Å and an outer diameter of 170 and 185 Å, respectively. The inner diameters of these models are close to the observed 100 Å; the smaller outer diameter (170 to 185 Å versus 200 Å)

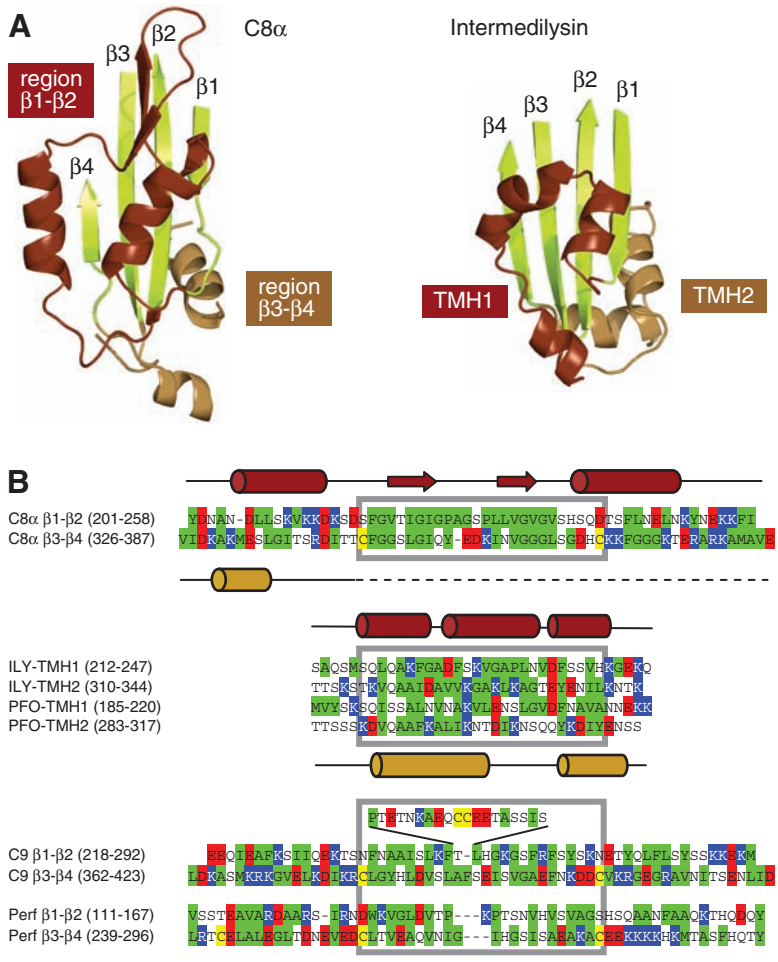

Fig. 2. Comparison of putative transmembrane regions. (**A**) Cartoon diagrams of domains d3 of C8α-MACPF (left) and intermedilysin (right). The putative β hairpin regions β1-β2 and TMH1 are colored in dark brown, and β3-β4 and TMH2 are colored in light brown. (**B**) Sequence alignment of (i) the β1-β2 and β3-β4 regions of C8α, C9, and perforin (Perf) and (ii) TMH1 and TMH2 of perfringolysin (PFO) and intermedilysin (ILY). Residues (*31*) are colored according to character: hydrophobic (green), positively charged (blue), negatively charged (red), and hydrophilic (white). Yellow indicates cysteine residues. Secondary structure elements, as observed for C8α-MACPF and intermedilysin, are indicated. Putative transmembrane regions are indicated by gray boxes.

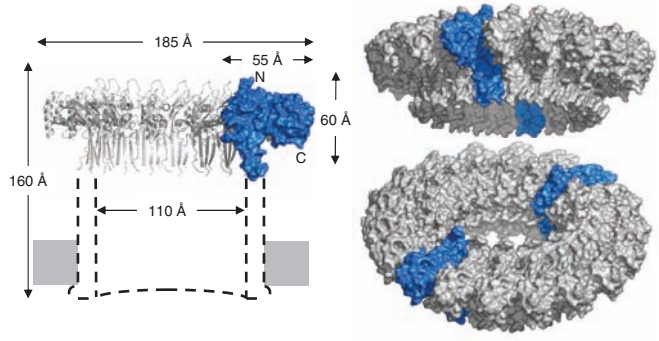

Fig. 3. Hypothetical model of the C9 pore. Shown is a pore model derived from a ring of 18 monomers of C8α-MACPF. (**Left**) Cross section of the pore, with MACPF domains forming the torus. (**Right**) Two orientations of the torus in surface representation, with two individual monomers highlighted (in blue) for convenience.

is possibly caused by the missing C-terminal domains that are connected to the outer rim of the torus. Thus, based on a MACPF domain, the main characteristics of the C9 pore can be modeled.

Membrane recognition and pore formation by the complement proteins depend on a sequential assembly of the MAC. The C8α-MACPF and C8β-MACPF domains are sufficient for a functional C5b–8 complex, indicating that the flanking N- and C-terminal domains in C8 are not essential for complex formation (*17*, *27*). The flanking domains, however, possibly cover the putative TMHs in soluble C8. Soluble forms of the cell-surface protein CD59 do not bind soluble C8 or C9 (*13*). CD59 binds residues 365 to 371 of C9 and residues 320 to 415 in C8α (*28*), which map to the TMH2 region. Presumably, docking of C8 or C9 onto the MAC reorients the flanking domains exposing the TMHs, which are subsequently "caught in the act" by CD59 present on host cells, and hence the membrane insertion is blocked. In CDCs, membrane insertion only takes place after oligomerization [that is, a large oligomeric prepore is formed on top of the membrane before the membrane is perforated (*26*)]. C8α inserts without oligomerization, which is consistent with the hydrophobic character of the putative TMHs. Partial and incomplete pores are observed, when limiting numbers of C9 are available for binding to C5b–8 (*11*). These data indicate that MAC pore formation is gradual and does not require oligomeric prepores. In this process, C8 plays an important role by binding to the membrane-bound C5b–7 complex, penetrating and destabilizing the membrane, thus readily enabling pore formation by C9.

Perforin, perhaps, acts more like CDCs. Membrane binding by perforin is Ca^{2+}-dependent and is mediated by its C-terminal C2 domain (*29*). The C2 fold is closely related to the fold of the C-terminal d4 domain in CDCs (fig. S5). Notably, the "undecapeptide" membrane–binding site in d4 overlaps with the Ca^{2+}-dependent binding site in C2, indicating a common orientation when bound to a membrane. Like in CDCs and C9, the putative TMHs of perforin are amphipathic in character. The amphipathic regions presumably do not penetrate the membrane easily. We argue that unassisted pore formation [as for CDCs, perforin, and in vitro poly(C9)] hence requires formation of a large oligomeric prepore on the membrane to facilitate perforation of the membrane.

The MACPF domain of complement proteins C6 to C9 and perforin is similar to domains d1 and d3 of bacterial CDCs. This finding indicates a possible common evolutionary origin and a common mechanism of membrane insertion. The structural insights could be valuable in the design of therapeutics preventing inappropriate activation of the terminal pathway of complement, as in the case of paroxysmal nocturnal hemoglobinuria and hyperacute rejection of transplanted organs.

References and Notes

1. M. J. Walport, *N. Engl. J. Med.* **344**, 1058 (2001).
2. M. J. Walport, *N. Engl. J. Med.* **344**, 1140 (2001).
3. R. Wurzner, A. Orren, P. J. Lachmann, *Immunodefic. Rev.* **3**, 123 (1992).
4. H. J. Muller-Eberhard, *Annu. Rev. Immunol.* **4**, 503 (1986).
5. A. F. Esser, *Toxicology* **87**, 229 (1994).
6. J. M. Sodetz, *Curr. Top. Microbiol. Immunol.* **140**, 19 (1989).
7. E. W. Steckel, B. E. Welbaum, J. M. Sodetz, *J. Biol. Chem.* **258**, 4318 (1983).
8. M. C. Peitsch *et al.*, *Mol. Immunol.* **27**, 589 (1990).
9. A. P. Gee, M. D. Boyle, T. Borsos, *J. Immunol.* **124**, 1905 (1980).
10. J. Tschopp, H. J. Muller-Eberhard, E. R. Podack, *Nature* **298**, 534 (1982).
11. J. Tschopp, *J. Biol. Chem.* **259**, 7857 (1984).
12. R. G. DiScipio, T. E. Hugli, *J. Biol. Chem.* **260**, 14802 (1985).
13. Y. Huang, F. Qiao, R. Abagyan, S. Hazard, S. Tomlinson, *J. Biol. Chem.* **281**, 27398 (2006).
14. E. R. Podack, G. Dennert, *Nature* **302**, 442 (1983).
15. G. Dennert, E. R. Podack, *J. Exp. Med.* **157**, 1483 (1983).
16. E. R. Podack, H. Hengartner, M. G. Lichtenheld, *Annu. Rev. Immunol.* **9**, 129 (1991).
17. D. J. Slade, B. Chiswell, J. M. Sodetz, *Biochemistry* **45**, 5290 (2006).
18. J. Rossjohn, S. C. Feil, W. J. McKinstry, R. K. Tweten, M. W. Parker, *Cell* **89**, 685 (1997).
19. G. Polekhina, K. S. Giddings, R. K. Tweten, M. W. Parker, *Proc. Natl. Acad. Sci. U.S.A.* **102**, 600 (2005).
20. S. J. Tilley, H. R. Saibil, *Curr. Opin. Struct. Biol.* **16**, 230 (2006).
21. R. K. Tweten, *Infect. Immun.* **73**, 6199 (2005).
22. K. S. Giddings, J. Zhao, P. J. Sims, R. K. Tweten, *Nat. Struct. Mol. Biol.* **11**, 1173 (2004).
23. M. W. Parker, S. C. Feil, *Prog. Biophys. Mol. Biol.* **88**, 91 (2005).
24. L. A. Shepard *et al.*, *Biochemistry* **37**, 14563 (1998).
25. O. Shatursky *et al.*, *Cell* **99**, 293 (1999).
26. S. J. Tilley, E. V. Orlova, R. J. Gilbert, P. W. Andrew, H. R. Saibil, *Cell* **121**, 247 (2005).
27. C. L. Brannen, J. M. Sodetz, *Mol. Immunol.* **44**, 960 (2007).
28. D. H. Lockert *et al.*, *J. Biol. Chem.* **270**, 19723 (1995).
29. I. Voskoboinik *et al.*, *J. Biol. Chem.* **280**, 8426 (2005).
30. W. L. Delano, The PyMOL Molecular Graphics System (DeLano Scientific, San Carlos, CA, 2002), http://pymol.sourceforge.net.
31. Single-letter abbreviations for the amino acid residues are as follows: A, Ala; C, Cys; D, Asp; E, Glu; F, Phe; G, Gly; H, His; I, Ile; K, Lys; L, Leu; M, Met; N, Asn; P, Pro; Q, Gln; R, Arg; S, Ser; T, Thr; V, Val; W, Trp; and Y, Tyr.

32. We thank T. H. C. Brondijk, B. J. C. Janssen, F. J. Milder, and L. Rutten for assistance, M. R. Daha, E. G. Huizinga and J. A. G. van Strijp for critically reading the manuscript. We thank the European Synchrotron Radiation Facility for providing synchrotron radiation facilities and the beamline scientists at ID-29 for their help with data collection. This work was supported by a "Pionier" grant (P.G.) of the Council for Chemical Sciences of the Netherlands Organization for Scientific Research. Coordinates and structure factors have been deposited in the Protein Data Bank (PDB) (www.rcsb.org) under accession code 2QQH.

Supporting Online Material

www.sciencemag.org/cgi/content/full/317/5844/1552/DC1
Materials and Methods
Figs. S1 to S5
Table S1
References

27 June 2007; accepted 3 August 2007
10.1126/science.1147103

Anti-Inflammatory Activity of Human IgG4 Antibodies by Dynamic Fab Arm Exchange

Marijn van der Neut Kolfschoten,[1] Janine Schuurman,[2] Mario Losen,[3] Wim K. Bleeker,[2] Pilar Martínez-Martínez,[3] Ellen Vermeulen,[1] Tamara H. den Bleker,[1] Luus Wiegman,[2] Tom Vink,[2] Lucien A. Aarden,[1] Marc H. De Baets,[3,4] Jan G.J. van de Winkel,[2,5] Rob C. Aalberse,[1]* Paul W. H. I. Parren[2]*

Antibodies play a central role in immunity by forming an interface with the innate immune system and, typically, mediate proinflammatory activity. We describe a novel posttranslational modification that leads to anti-inflammatory activity of antibodies of immunoglobulin G, isotype 4 (IgG4). IgG4 antibodies are dynamic molecules that exchange Fab arms by swapping a heavy chain and attached light chain (half-molecule) with a heavy-light chain pair from another molecule, which results in bispecific antibodies. Mutagenesis studies revealed that the third constant domain is critical for this activity. The impact of IgG4 Fab arm exchange was confirmed in vivo in a rhesus monkey model with experimental autoimmune myasthenia gravis. IgG4 Fab arm exchange is suggested to be an important biological mechanism that provides the basis for the anti-inflammatory activity attributed to IgG4 antibodies.

In the classic paradigm, immunoglobulins represent products of clonal B cell populations, each producing antibodies recognizing a single antigen specificity (*1*, *2*). Human immunoglobulin G (IgG) antibodies exist in four subclasses with distinct structural and functional properties. IgGs are composed of two heavy chain–light chain pairs (half-molecules), which are connected via inter–heavy chain disulfide bonds situated in the hinge region, as well as by noncovalent bonds mostly situated between the third constant (C_H3) domains (*3*). Stability of the inter–heavy chain disulfide bonds varies between subclasses, and for IgG4 in particular, intra–heavy chain disulfide bonds may be formed instead (*4*).

IgG4 antibodies differ functionally from other IgG subclasses in their anti-inflammatory activity, which includes a poor ability to induce complement and cell activation because of low affinity for C1q (the q fragment of the first component of complement) and Fc receptors (*5*, *6*).